STUDIES OF THE REACTION OF CHF_3 WITH METHANE

Hai Yu, Eric M. Kennedy [*], John C. Mackie
and Bogdan Z. Dlugogorski
Process Safety and Environment Protection Research Group
School of Engineering
The University of Newcastle, Callaghan, NSW 2308, Australia
Fax: (+61 2) 4921 6920; Tel: (+61 2) 4921 6177; Email: eric.kennedy@newcastle.edu.au

Abstract

The motivation behind the study is that reaction of CHF_3 with CH_4 provides a possible route for synthesis of $CH_2=CF_2$ ($C_2H_2F_2$). Experiments are carried out in a plug flow, isothermal α-alumina reactor at atmospheric pressure over the temperature range of 973 to 1173 K. Under all conditions studied for the reaction of CHF_3 and CH_4, the major products are C_2F_4, $C_2H_2F_2$ and HF. The initial step is the gas-phase unimolecular decomposition of CHF_3, producing CF_2 and HF. It is proposed that CF_2 decomposes on the surface of *α*-alumina, producing F radicals that are responsible for the activation of CH_4. A reaction scheme developed on the basis of the existing NIST HFC and GRI-Mech 3.0 mechanisms is used to model the reaction of CHF_3 with CH_4. Generally satisfactory agreement between experimental and modelling results is obtained on the conversion levels of CHF_3 and CH_4 and rates of formation of major products.

Introduction

Hydrofluorocarbons (HFCs) have been generally viewed as environmentally acceptable alternatives to CFCs and halons, as HFCs do not contain Cl or Br atoms and hence have an ozone depletion potential of zero. In the last two decades, the amount of HFCs used as alternatives to CFCs and halons has been increasing. The global HFC demand is projected to increase 14% annually through 2007 to almost 600,000 metric tonnes (*1*). Unfortunately, HFCs are themselves synthetic greenhouse gases (GHGs), with long atmospheric lifetimes. For example, CHF_3 (HFC-23) is currently used as a substitute for CFC refrigerants and halon fire extinguishing agents as well as in the semiconductor industry. It is an unintended by-product of HCFC-22 ($CHClF_2$) manufacture. It is estimated to have an atmospheric lifetime of 264 years and has a global warming potential (GWP) of 12,000 (*2*). The implementation of the *Kyoto Protocol* will inevitably result in the stockpiling of vast quantities of HFCs for disposal, which will further intensify research efforts aimed at developing technologies for treatment of not only ODSs but also HFCs.

Compared to the intensive research effort on the treatment of halon and CFC, very limited research has been focused on the development of technologies for treatment of HFCs including CHF_3, especially on the conversion technologies which aim to transform a large amount of byproduct HFCs into valuable and environmentally benign products. Moon et al have studied the thermal pyrolysis of a mixture of CHF_3 and C_2F_4 under the conditions of reaction temperatures of 970-1173 K, residence times of 0.01-14 s, and CHF_3/C_2F_4 ratios of 0.1-5 and found that the reaction can be used to produce hexafluoropropylene ($CF_3CF=CF_2$) effectively and selectively (*3*). Recently Tosoh F-TECH Inc. has developed a new and patented technology for the manufacture of CF_3I via the catalytic reaction of CHF_3 and I_2 over alkali metal salts (*4*).

We have recently reported the results of an experimental investigation of the gas phase reaction of CH_4 with CFC-12 (CCl_2F_2) and halon 1211 ($CBrClF_2$) respectively, and found that both reactions can give high yields of the coupling products $C_2H_2F_2$ at elevated temperatures (*5,6*). $C_2H_2F_2$ is a highly valuable feedstock and is in high demand. It is widely used in the fluoroelastomer and semiconductor industries. For example, it is the key monomer for the synthesis of a variety of products, most notably poly(vinylidene fluoride) (PVDF), Viton® (produced by Dupont Corporation) and KEL-F® (produced by 3M).

In this study, we report results of experimental and computational studies of reaction of CHF_3 with CH_4. The purpose of this study is to investigate the thermal reaction of CHF_3 with CH_4 as a possible option for the conversion of CHF_3 to $CH_2{=}CF_2$ and to gain an understanding of the reaction chemistry involved.

Experimental Section

The experimental facility used in this study has been described in detail elsewhere (*7,8*). Reactions carried out in this study include reaction of CHF_3 (>98%, Sigma) with CH_4 (99.99%, Linde) and pyrolysis of CHF_3, CH_4 and $CHClF_2$ (>99%, Actrol) in N_2 (99.999%, Linde). Reaction conditions are summarised in Table 1.

Table 1 Summary of reaction conditions studied in this investigation (*P* = 1.01 bar; Reactor volume = 1.35 cm^3)

Condition	Reaction	Input molar flow rate mmol/h	*T*, K
1	$CHF_3 + CH_4$	N_2:150 CH_4: 14.0 CHF_3 12.9	973-1173
2	$CHF_3 + CH_4$	N_2: 150 CH_4: 14.0 CHF_3: 6.6	1153
3	CHF_3 pyrolysis	N_2: 150 CHF_3: 12.9	973-1173
4	CH_4 pyrolysis	N_2:150 CH4 12.9	973-1173
5	$CHClF_2$ pyrolysis	N_2: 150 $CHClF_2$: 8.2	773-1023

The conversion of reactants, X_i, and rate of formation of product, F_j, are calculated according to the following equations:

$$X_i = \frac{f_{i,\ \mathrm{in}} - f_{i,\ \mathrm{out}}}{f_{i,\ \mathrm{in}}} \times 100\%$$

$$F_j = f_{j,\ \mathrm{out}}$$

where $f_{i,\ \mathrm{in}}$, $f_{i,\ \mathrm{out}}$ and $f_{j,\ \mathrm{out}}$ denote molar flowrates of reactant *i* in the feed, reactant *i* at the outlet, and product *j* at the outlet, respectively.

Characterisation

X-ray diffraction patterns of the fresh and used α-Al_2O_3 and AlF_3 samples were obtained on a Philips Powder X-ray diffractomer (PW 1710) using CuK*α* radiation (Ni filter**)** under a voltage of 40 kV and an intensity of 30 mA.

BET surface area of fresh *α*-Al_2O_3 and *β*-$AlF_3 \cdot 3H_2O$ (Sigma) was measured on AutoChem 2910 from Micromeritics. A 30% N_2/He (Linde) was used as adsorption gas with He as carrier gas for TCD.

Chemical Kinetic Modelling

The gas phase reaction of CHF_3 with CH_4 was modelled using a commercial software package Chemkin Collection 3.7.1 in which, PLUG is used to model the gas phase reaction in the tubular reactor and Aurora for the analysis of reaction pathway in the well-mixed batch reactor (*9*). Since the reaction is carried out in the highly diluted system, the results obtained from both plug flow and well mixed batch reactors are very similar.

Results and Discussion

The reaction of CHF_3 with CH_4 commences at 1023 K, under condition 1 listed in Table 1. The major products are C_2F_4, $CH_2{=}CF_2$ ($C_2H_2F_2$) and HF under all conditions studied. Minor products include C_2H_2, C_2H_4, C_2H_3F, C_2HF_3 and CO_2. C_2H_6, CH_2F_2 and CHF_2CHF_2 are detected in trace amounts. Some unidentified species produced at high temperatures are quantified, assuming that their response factors are equal to that of $C_2H_2F_2$. Coke has been observed on the internal surface of the reactor and thermocouple sheathes. It has also been found that unidentified materials are deposited on the inner surface of Teflon tubes which are used to connect reactor to the acid trap and also in the caustic solutions. We suggest that these solid species are polymeric materials formed via the polymerisation of unsaturated products, mainly C_2F_4 or $C_2H_2F_2$. It should be pointed out that the formation of CO_2 is unexpected. We have determined that the amount of oxygen in the feed (CH_4, CHF_3 and N_2) is below the MicroGC detection limit (less than 10 ppm) and such a low concentration would be unlikely to generate the amounts of CO_2 detected as a consequence of reaction. We suggest that oxygen arises from the *α*-alumina, the material of reactor and thermocouple sheath. This will be discussed later.

Figure 1 shows the conversion of CHF_3 and CH_4, and rate of production of major products as a function of time on stream in a fresh alumina tube at 1153 K under condition 2 listed in Table 1. The experiment was repeated under the same condition using the same tube (called the "used tube") and results are also included in Figure 1 for comparison.

As can be seen in Figure 1, when a fresh tube is used, the conversion of CHF_3 and CH_4 remains relatively unchanged and the rate of formation of $C_2H_2F_2$ decreases slightly with time on stream while the rates of formation of C_2F_4 and HF increase significantly before reaching relatively steady values (more than 2 h on stream). This phenomenon was less obvious when the experiment was repeated using the used alumina tube. The rates of formation of C_2F_4 and HF attain steady values in a relatively short period (less than 2 h). The steady state conversion level and rate of production of major products are very similar in both cases (fresh and used tubes).

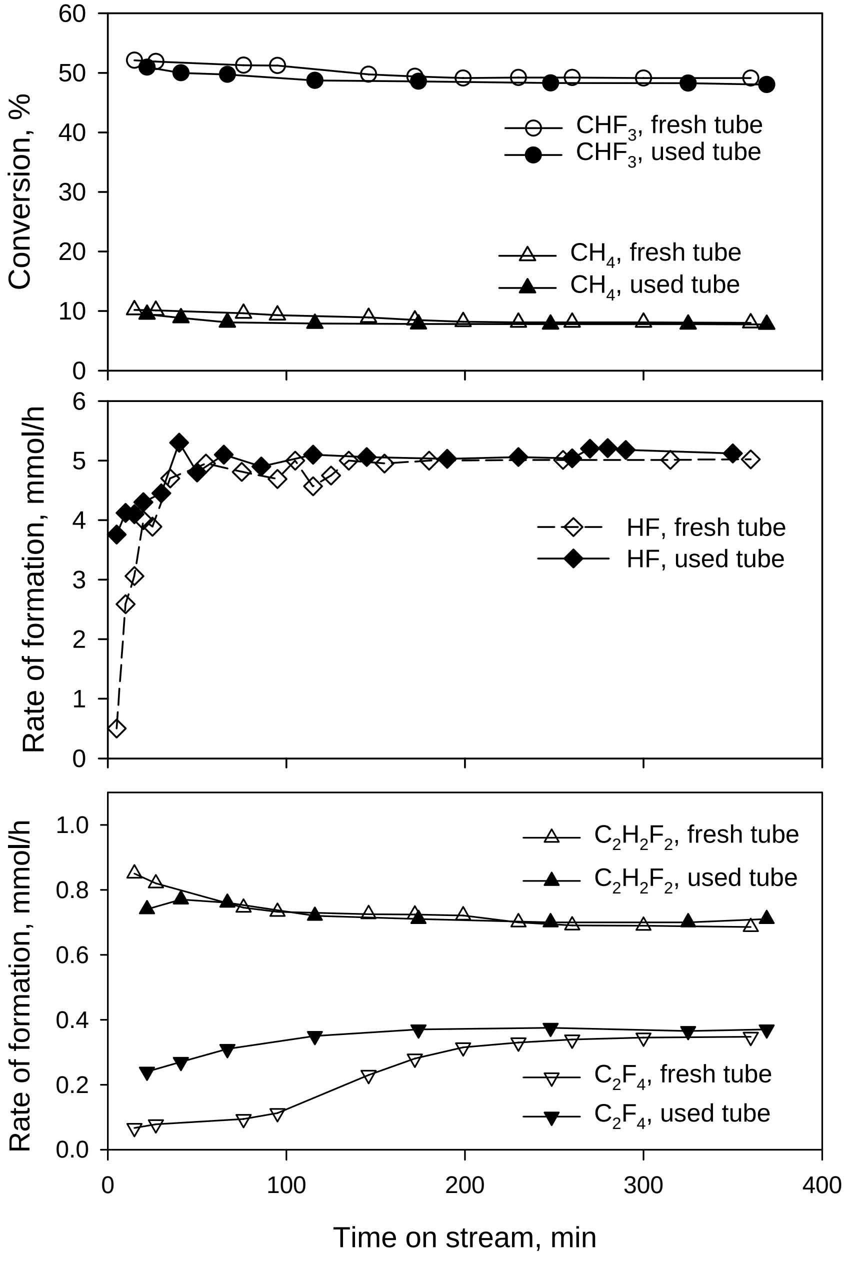

Figure 1 Conversion of CH_4 and CHF_3 and rates of formation of major products as a function of time on stream during the reaction of CHF_3 with CH_4 in fresh and used α-alumina reactors under condition 1 (see Table 1).

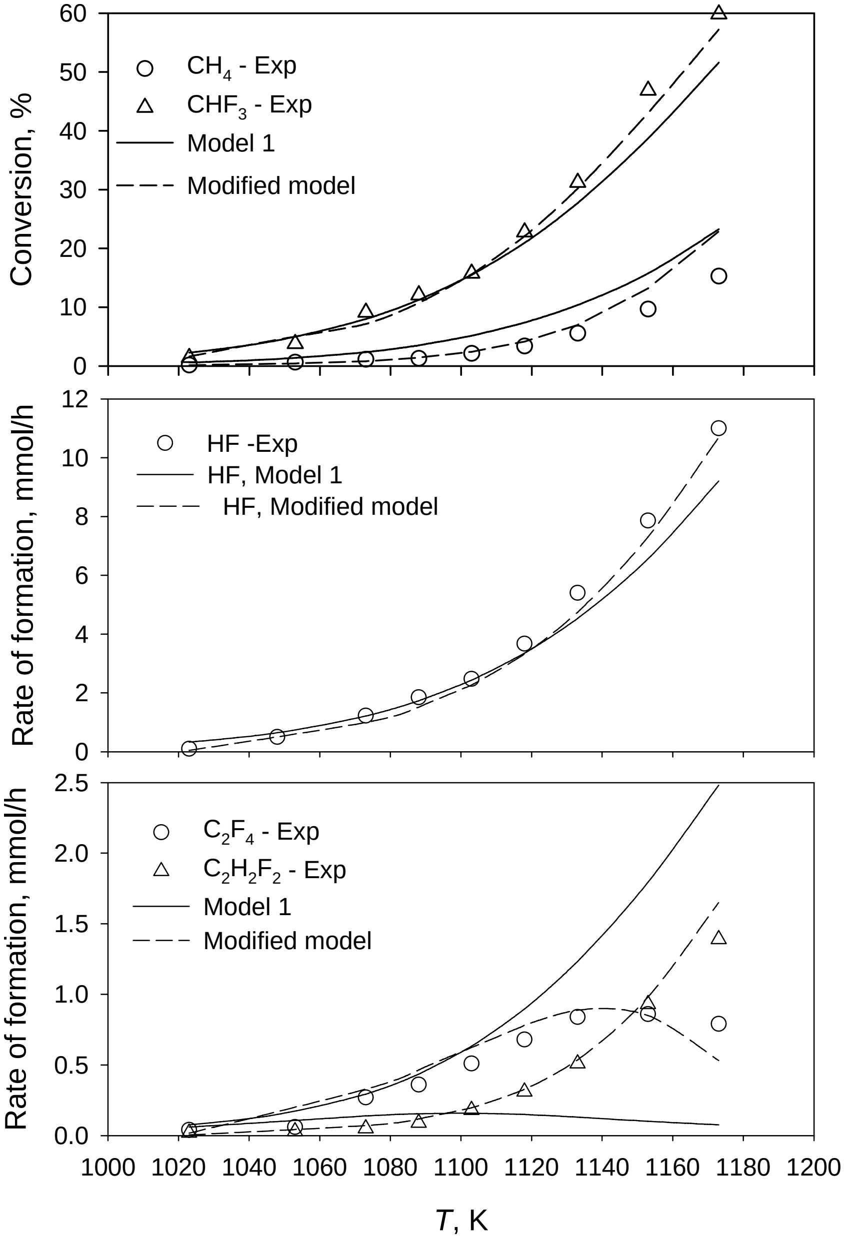

Figure 2 Comparison of conversion of CH_4 and CHF_3 and rates of formation of major products as a function of temperature under condition 1 (see Table 1).

A similar behaviour is observed for the reaction of CHF_3 with CH_4 under other reaction conditions studied in this investigation. Unless stated otherwise, the results (conversion level and rate of formation of products) presented in this paper are obtained in the alumina tube which is pretreated under condition 1 at 1173 K for 6 h.

With increase with temperature, the conversion levels of both CH_4 and CHF_3 increase, as expected (Figure 2). The rates of formation of all products except C_2F_4 increase with temperature while the rate of formation of C_2F_4 increases with temperature to 1153 K above which the rate starts to decline. The mass balance of hydrogen is relatively constant and generally over 98% of hydrogen is recovered, while mass balances of carbon and fluorine deteriorate with temperature, suggesting that elemental difference is a consequence of the formation of coke and polymeric materials comprising carbon and fluorine containing materials (Results are not included in the paper).

Although $C_2H_2F_2$ is produced as a major product, both the yield and selectivity to $C_2H_2F_2$, the target product, are generally low, being 7.2 and 15.4% respectively at 1153 K under condition 1 (Table 1). . Increase in ratio of CH_4/CHF_3 in the feed can increase both yield and selectivity at a similar conversion level of CHF_3 (as shown in Table 2), but only moderately.

Table 2 Effect of input CH_4/CHF_3 ratio on the yield and selectivity to $C_2H_2F_2$ (T = 1153 K).

Reaction condition	Ratio of CH_4/CHF_3	CH_4 conv %	CHF_3 conv %	Yield to $C_2H_2F_2$ %	Selectivity to $C_2H_2F_2$ %
1	1.1	9.67	46.8	7.2	15.4
2	2.1	7.75	48.0	11	22.4

Yield of $C_2H_2F_2$ = 100 • $f_{C_2H_2F_2,out} / f_{CHF_3,in}$; selectivity of $C_2H_2F_2$ = 100 • $f_{C_2H_2F_2,out} / (f_{CHF_3,in} - f_{CHF_3,out})$

To enhance both yield and selectivity to $C_2H_2F_2$, it is of importance to understand the reaction mechanism involved in this novel chemistry.

Mechanistic analysis

The experiments on the pyrolysis of CHF_3 and CH_4 diluted in N_2 have been carried out under condition 3 and 4 respectively. There is no reaction occurring in the case of pyrolysis of CH_4 at 973-1173 K, while at 1023 K, CHF_3 starts to decompose, producing C_2F_4 and HF as major products. The reaction of CHF_3 with CH_4 commences at a similar temperature, suggesting that the initial reaction involves the decomposition of CHF_3. Thermal decomposition of CHF_3 has been investigated by several researchers with the results indicating the predominant pathway for the initial decomposition of CHF_3 is via (R1) which has an activation energy in the range of 230-289 kJ/mol (*3,10*).

$$CHF_3 \rightarrow CF_2 + HF \qquad \Delta H^{o}_{f,\ 298} = 238 \text{ kJ/mol} \qquad \text{(R1)}$$

Fully fluorinated products C_2F_4 and C_3F_6 are formed via the combination of CF_2 (R2) and (R3).

$$CF_2 + CF_2 \rightarrow C_2F_4 \qquad \text{(R2)}$$
$$C_2F_4 + CF_2 \rightarrow C_3F_6 \qquad \text{(R3)}$$

The formation of CH_2=CF_2 should involve the activation of CH_4. To elucidate the reaction pathways leading to the activation of CH_4 and formation of CH_2=CF_2, the existing NIST HFC and GRI-Mech 3.0 mechanisms are assembled and initially used to model the reaction of CHF_3 with CH_4 (*11,12*). Since the concentration of oxygen in the feed is negligible, species and reaction sets containing oxygen are removed from the two reaction schemes and resultant mechanism include 63 species and 345 reactions. This is Model 1.

Figure 2 show the comparison of conversion of CH_4 and CHF_3 and rates of formation of major product as a function of temperature during the reaction of CHF_3 with CH_4 under condition 1.

Model 1 does not produce results which fit the experimental results very well, although it does predict a relatively high conversion level of CH_4 and production of $C_2H_2F_2$ as a major product. The reaction pathway analysis of Model 1 using Aurora suggests that the activation of CH_4 primarily involves the reverse reactions of (R4) and (R5), and forward reaction (R6) coupled through CF_3.

$$CHF_2 + CH_3 \rightarrow CF_2 + CH_4 \qquad \text{(R4)}$$
$$CF_3 + CHF_2 \rightarrow CF_2 + CHF_3 \qquad \text{(R5)}$$
$$CF_3 + CH_4 \rightarrow CHF_3 + CH_3 \qquad \text{(R6)}$$

There are, however, major problems with the acceptance of the rate constants of reactions (R4) and (R5) as presently contained in the NIST HFC mechanism. Firstly, if the reverse rate constants for reactions (-R4) and (-R5) are calculated from the NIST values using the accepted thermochemistry, *A*-factors of 8×10^{14} and 4×10^{14} cm^3 mol^{-1} s^{-1} are obtained, respectively. There do not appear to be any reported observations of H abstraction from saturated compounds by CF_2. The very low reactivity of CF_2 with molecules has also be confirmed by Battin-Leclerc et al who experimentally studied the reaction of CF_2 with many molecules including CH_4, O_2, CH_4 and C_2H_4 at temperatures 295-873 K (*13*). No reaction was observed between CF_2 and any of the molecules studied in their investigation. (Battin-LeClerc et al set an upper limit for the rate constant of (-R8) of $<4\times10^{-5}$ cm^3 mol^{-1} s^{-1} at 873 K.) Furthermore, based on transition state theory, and assisted by an evaluation of the available experimental data in the literature, Benson proposed that most of pre-exponential factors for radical-molecule metathesis reactions (not involving atoms) are $10^{11.5\pm0.5}$ cm^3 mol^{-1} s^{-1} under reaction conditions similar to those in our investigation (*14*). Additionally, in the course of our quantum chemical studies (15) on the mechanism of reaction between CF_2 and CH_3, we were unable to locate an abstraction transition state for reaction of CF_2 with either CH_4 or CHF_3. Instead, we believe that the products of reaction between CHF_2 + CH_3 and CF_3 + CHF_2 would most likely be the saturated recombination products CH_3CHF_2 and CF_3CHF_2.

Thus, reactions (-R4), (-R5) and (R6) are not likely to be responsible for CH_4 activation. In order to further examine the possible reactions involved with CH_4 activation, we estimated the kinetic parameters for (-R4) and (-R5) and replaced reactions (R4) and (R5) in the NIST HFC and GRI-Mech 3.0 mechanisms with

$$CF_2 + CH_4 \rightarrow CHF_2 + CH_3 \quad k\ (\text{cm}^3\text{mol}^{-1}\text{s}^{-1}) = 10^{13}\exp(-160\ \ \text{kJ mol}^{-1}/RT) \qquad \text{(-R4)}$$
$$CF_2 + CHF_3 \rightarrow CF_3 + CHF_2 \quad k\ (\text{cm}^3\text{mol}^{-1}\text{s}^{-1}) = 10^{13}\exp(-178\ \ \text{kJ mol}^{-1}/RT) \qquad \text{(-R5)}$$

The activation energies for (-R4) and (-R5) are assumed to be 160 and 178 kJ/mol respectively, which are standard enthalpy changes of these two reactions at 298 K, and these values are expected to be lower than the actual activation energies under the higher temperature reaction conditions. The pre-exponential factors are assumed to be 10^{13} (cm^3 mol^{-1} s^{-1}) which is substantially higher than that of similar reactions (radical-molecule metathesis reactions).

CH_3, generated principally from (R6), reacts with CF_2, forming $C_2H_2F_2$ via (R7)

$$CH_3 + CF_2 \rightarrow CH_2{=}CF_2 + H \qquad \Delta H^{o}_{f,\ 298} = -77.5 \text{ kJ/mol} \qquad \text{(R7)}$$

A detailed quantum chemical study of reaction of CF_2 with CH_3 (R7) presented elsewhere, suggests that this reaction can lead to the formation of $C_2H_2F_2$ with an activation energy of almost zero and takes place rapidly (*15*). Our modified model comprises revised reactions (-R4), (-R5) and (R7) together with the other reactions in the NIST HFC and GRIMech 3.0 mechanisms. The new modelling results show that there is virtually no CH_4 converted (despite the large *A*-factors for (-R4) and (-R5)) and the predicted reaction is simplified to the pyrolysis of CHF_3. We therefore suggest that there are other steps which contribute to the activation of CH_4.

The dynamic behaviour displayed during the reaction, especially during the initial few hours, indicates that there are reactions occurring on the surface of the reactor and that CH_4 activation takes place as a consequence of surface reactions. In order to assess the extent of surface reaction, a transient study of the reaction of CHF_3 and CH_4 was conducted under condition 2 (Table 1). After a period of 70 min when the reaction reached a steady state, the CHF_3 flow was terminated while flowrates of CH_4 and dilution gas nitrogen in the feed were kept unchanged. As shown in Figure 3, the flowrate of CHF_3 at the outlet rapidly dropped to zero and the flowrate of CH_4 increased to the input level. The rate of formation of all products except C_2H_6 decreased below detection limit in a short period time following a pattern similar to that of CO_2. Interestingly, the amount of C_2H_6 produced, although low, increased slightly before it eventually dropped. This suggests the formation of CH_3 as an intermediate during the activation of CH_4. In the presence of CHF_3, CH_3, produced after the cleavage of a C-H bond in CH_4, will more likely react with CF_2 or other species, while in the absence of CHF_3, the possibility for recombination of CH_3 will be relatively high. As a result, the amount of C_2H_6 increases slightly, as observed.

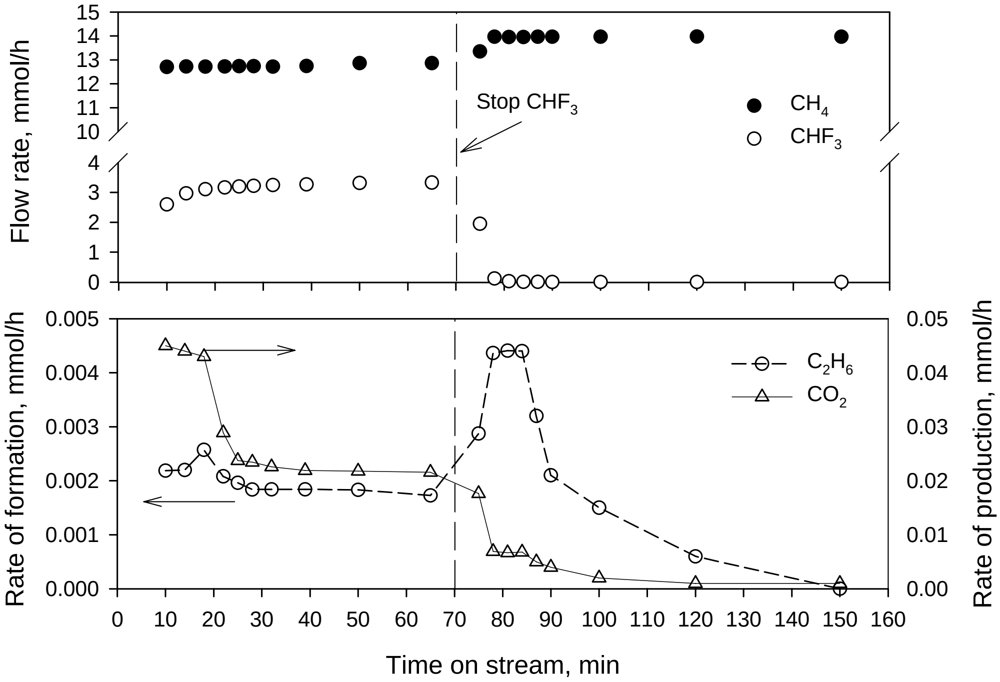

Figure 3 Results of transient study of reaction of CHF_3 and CH_4 at 1153 K under condition 2 (see Table 1).

To facilitate our understanding of the effect of the reactor surface, we investigated the reaction of CHF_3 with CH_4 under condition 2 in the presence of α-alumina particles which are prepared by crushing a fresh alumina tube and sieving particles to the range of 90-325 μm. Alumina particles of 0.2 g, having a bulk volume of 0.08 cm^3 and surface area of 380 cm^2 were charged into the reactor (the inner surface area of the reaction zone is estimated to be less than 10 cm^2). The alumina reactor is pre-treated under conditions described previously in order to minimize the effect of the fresh alumina surface. The length of reaction zone is increased accordingly in order to keep the void volume of the reactor and thus residence time approximately the same as when an empty tube is used. The results show that, the conversion level of CHF_3 is relatively unchanged compared to that obtained in the absence of alumina particles while the conversion of CH_4 is slightly higher. The product profiles as a function of time on stream show a pattern similar to that observed when the fresh tube is used. The formation of C_2F_4 increased with time on stream. At steady state, the rate of formation of C_2F_4 is slightly lower while the rate of production of $C_2H_2F_2$ is slightly higher. It should be pointed out that a relatively large amount of CO_2 is released in the initial 30 min on stream after which the amount of CO_2 decreased dramatically and reached a relatively low steady value.

The formation of CO_2 involves both the release of O from the alumina support and the complete cleavage of C-F and C-H bonds in some species present in the reaction system. XRD analysis of fresh and used alumina in the reaction of CHF_3 and CH_4 shows that a new phase appears in the used alumina particles and is identified as α-AlF_3 (Figure 4). This suggests that the alumina chips have undergone fluorination, which should also happen to the surface alumina on the alumina tube. It has been found that the fluorination of alumina occurs only after CHF_3 decomposes into

CF_2 + HF at temperatures above 1023 K. We therefore suggest that HF and/or CF_2 play a dominant role in the fluorination.

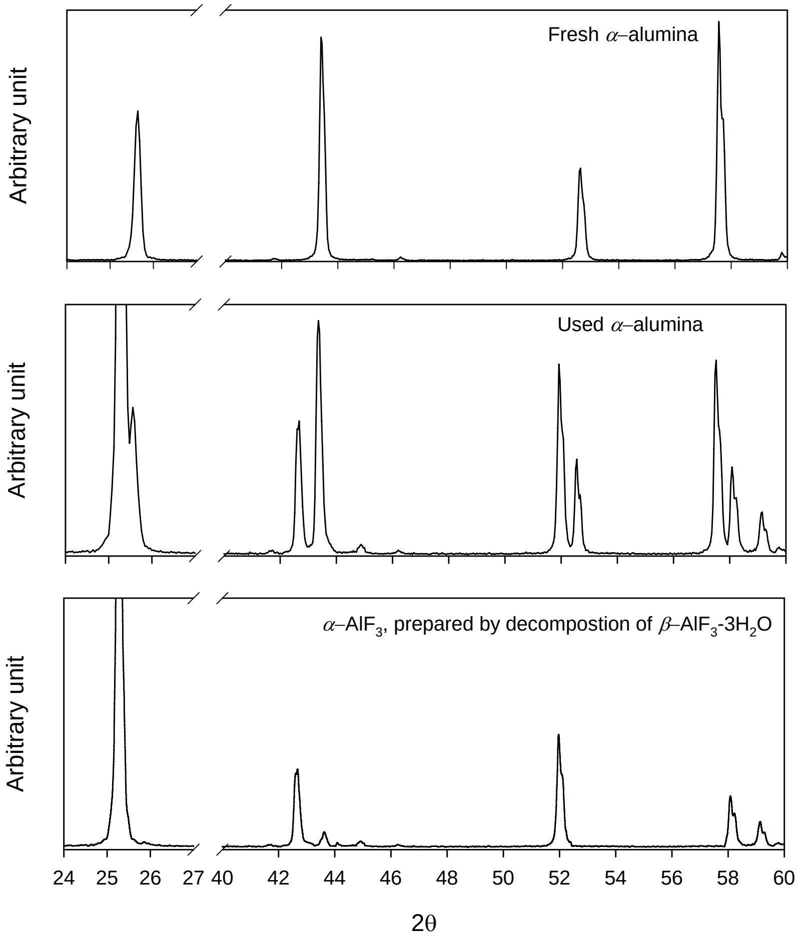

Figure 4 XRD spectra of fresh α-alumina, α-alumina used in the reaction of CHF_3 with CH_4 under condition 2 (see Table 1), and β-$AlF_3 \cdot 3H_2O$ pretreated in nitrogen flow at 1153 K for 6h.

It has been documented (*16*) that α-alumina can be fluorinated by HF. However, the concurrent production of CF_2 and HF from the decomposition of CHF_3 makes it difficult to determine whether or not CF_2 plays a role in modifying the alumina during reaction. To determine the effect of CF_2 on fluorination of alumina, we investigated the pyrolysis of $CHClF_2$ in the presence of α-alumina chips (0.2 g) under condition 5 (see Table 1). It is generally agreed that the gas phase decomposition of $CHClF_2$ follows an HCl molecular elimination pathway, leading to formation of CF_2 and HCl. The extent of direct cleavage of either C-Cl or C-F bonds is negligible at least at temperatures studied in this investigation due to their high energy barriers. It has been reported that $CHClF_2$ molecule can chemically adsorb on γ-alumina, resulting in the cleavage of C-F bond and consequently fluorination of alumina at temperatures above 450 K (*17*). The fluorinated alumina then acts as catalyst for the dismutation reaction, leading to formation of CHF_3 and $CHCl_3$ as major products (R8).

$$3CHClF_2 \xrightarrow{\gamma\text{-}Al_2O_3} 2CHF_3 + CHCl_3 \qquad (R8)$$

However there is no report in the literature that α-alumina can be fluorinated by CFC and HFC molecules. Under the conditions studied in our investigation, the major products from the pyrolysis of $CHClF_2$ over α-alumina are C_2F_4 and HCl. Minor products include C_3F_6 and CO_2. CHF_3 is detected only in trace amounts. In addition, the fluorination of α-alumina is observed only at temperatures above 873 K at which the decomposition of $CHClF_2$ commences, generating CF_2 and HCl. This suggests that the fluorination is mostly likely ascribed to the presence of CF_2. Higher temperatures lead to a higher concentration of CF_2 during reaction and it is expected that more alumina is fluorinated. This is confirmed in the XRD spectra of alumina samples used in the pyrolysis of $CHClF_2$ at three different temperatures (823, 923 and 1023 K) (XRD patterns are not included). We then can conclude that not only HF but also CF_2 can play a role in fluorination of α-alumina. The interaction of CF_2 with the support can result in the cleavage of C-F bond in CF_2, producing C atom on the surface. Fluorination of alumina will lead to the replacement of O in alumina by F from both HF and CF_2. The formation of CO_2 is most likely ascribed to the interaction of C and O on the surface of fluorinated alumina. The interaction of alumina with CF_2 and HF can at least partially explain observed changes of C_2F_4 and HF concentrations with time on stream. In the initial several hours of reaction, more CF_2 and HF will react with the fresh surface of the alumina. As a result, the amount of C_2F_4, formed from the coupling of CF_2 decreased and so did the amount of HF in the product stream. The interaction of CF_2 with the support is enhanced with temperature as supported by increase in the amount of CO_2 formed and increasing mass losses at higher temperatures.

As the alumina is fluorinated into α-AlF_3, it is possible that the resultant α-AlF_3 is the active phase for CH_4 activation. To examine the possible role of α-AlF_3 on the reaction, a study of pyrolysis of CH_4, and the reaction of CHF_3 with CH_4, was conducted in the presence of α-AlF_3 under conditions 3 and 2 respectively. The α-AlF_3 is prepared in situ by heating 0.2 g β-$AlF_3 \cdot 3H_2O$ (having a bulk volume of 0.35 cm^3 and surface area of 480 cm^2) in nitrogen flow at 1153 K for 6 hours. As shown in Figure 4, the sample β-$AlF_3 \cdot 3H_2O$ has converted to α-AlF_3 after higher temperature treatment, behaviour consistent with that reported in the literature *(18)*. The results suggest that AlF_3 is not the active phase for the activation of CH_4 (Results are not included). This conclusion is also consistent with our transient study of CHF_3 with CH_4 as described previously. The formation of C_2H_6 after stopping flow of CHF_3 in the feed cannot be sustained even though the surface of the alumina has been fluorinated.

Although the experimental results suggest that the activation of CH_4 is related to the surface material, it is not clear how it is activated. The experimental results (formation of CO_2 and fluorination of alumina) suggest that the cleavage of C-F bonds in CF_2 occurs on the surface. We propose that fluorine radicals generated from the decomposition of CF_2 play different roles during reaction. Some of the fluorine radicals, similar to F from HF, can chemically adsorb on positively charged Al cations on the surface, forming stable F-Al bonds (fluorination of Al_2O_3). The fluorinated Al_2O_3 is not the active phase for activation of CH_4, as suggested by the experimental results of the reaction of CHF_3 and CH_4 in the presence of AlF_3. However, some fluorine atoms can react with CH_4 on the surface or after desorbing into the gas phase, producing CH_3. Such an activation step seems to be a weak function of surface area since the introduction of 0.2 g α-alumina to the reactor significantly increases the surface area from less than 10 cm^2 to ca. 380 cm^2 while the effect on the conversion level and product profile is only marginal. Based on the above discussion, we introduce into the existing mechanisms a simplified gas phase reaction step (R9) to mimic the surface reaction and/or desorption.

$$CF_2 \rightarrow F + F + C \qquad (R9)$$

Table 3 The modified and new reaction steps in the modified reaction scheme.

No.	Reaction	Forward reaction			References
		A	*n*	*E*	
		3.4E30	-4.0	288.7	
R1	$CHF_3 \rightarrow CF_2 + HF$		change to		
		2.8E13	0.0	288.7	*(3)*
R9	New reaction $CF_2 \rightarrow C + F + F$	2.8E10	0.0	205.0	This study
R3	New reaction $CF_2 + C_2F_4 \rightarrow C_3F_6$	1.6E11	0.0	77.0	*(19)*
		6.0E12	0.0	14.6	
R7	$CF_2 + CH_3 \rightarrow CH_2{=}CF_2 + H$		change to		
		2.1E13	-0.2	0.0	*(15)*
R4	$CHF_2 + CH_3 \rightarrow CF_2 + CH_4$	3.0E13	0.0	3.4	
	Change to				This study
-R4	$CF_2 + CH_4 \rightarrow CHF_2 + CH_3$	1.0E13	0.0	159.5	
R5	$CHF_2 + CF_3 \rightarrow CHF_3 + CF_2$	3.0E13	0.0	8.4	
	Change to				This study
-R5	$CF_2 + CHF_3 \rightarrow CHF_2 + CF_3$	1.0E13	0.0	168.8	

The rate coefficients of the forward reaction is $k = AT^n\exp(-E/RT)$ where A is in s^{-1}, or $cm^3\ mol^{-1}\ s^{-1}$, as appropriate, the activation energy is in kJ mol^{-1} and R is the ideal gas constant.
A software package (THERM) (*20*) was used to generate the polynomial coefficients for the new species C_3F_6 whose standard state enthalpy, standard state entropy and temperature dependant heat capacities are obtained from (*21*).

Other reaction steps are also introduced or modified, as shown in Table 3. The kinetic data for the decomposition of CHF_3 (R1) are adopted from Ref. 3 as these parameters give better agreement between modelling prediction and experimental results for pyrolysis of CHF_3 in nitrogen. It has been found that by optimising the kinetic parameters for (R9), a better agreement with the experimental data can be obtained, as shown in Figure 2.

Using the modified reaction scheme, the rate of production analysis is conducted and the reaction pathways leading to the formation of important products under conditions studied are summarised below.

$CHF_3 \rightarrow CF_2 + HF$ (initial step) (R1)
$CF_2 + CF_2 \rightarrow C_2F_4$ (Formation of C_2F_4) (R2)
$C_2F_4 + CF_2 \rightarrow C_3F_6$ (Formation of C_3F_6) (R3)
$CF_2 \rightarrow C + F + F$ (R9)
$F + CH_4 \rightarrow CH_3 + HF$ (Activation of CH_4) (R10)
$C + CH_3 \rightarrow C_2H_2 + H$ (Formation of C_2H_2) (R11)

$CH_3+CF_2 \rightarrow CH_2=CF_2 + H$ (Formation of $C_2H_2F_2$) (R7)
$C_2F_4 + H \rightarrow CF_2 + CHF_2$ (R12)
$CF_2 + H \rightarrow CF + HF$ (R13)
$CF + CH4 \rightarrow CH_2:CHF + H$ (Formation of C_2H_3F) (R14)
$CH_3 + CHF_2 \rightarrow CH_2:CHF + HF$ (Formation of C_2H_3F) (R15)
$CHF_2 + CHF_2 \rightarrow CHF_2\text{-}CHF_2$ (R16)
$CHF_2\text{-}CHF_2 \rightarrow CHF:CF_2 + HF$ (Formation of C_2HF_3) (R17)
$CHF_2 + CHF_2 \rightarrow CHF:CF_2 + HF$ (Formation of C_2HF_3) (R18)
$CHF_2 + CHF_2 \rightarrow CH_2F_2 + CF_2$ (Formation of CH_2F_2) (R19)
$C + H_2 \rightarrow CH + H$ (R20)
$CH + CH_4 \rightarrow H + C_2H_4$ (Formation of C_2H_4) (R21)
$CH_3 + CH_3 \rightarrow C_2H_6$ (Formation of C_2H_6) (R22)

The proposed reaction step (R9) plays a key role in the modified reaction scheme. F generated from this step is responsible for the activation of CH_4 and resultant CH_3 then reacts with CF_2 (R7) and C (R11) to produce $C_2H_2F_2$ and C_2H_2. Since the activation of CH_4 is achieved at the expense of decomposition of CF_2, as a result, less CF_2 is available for the reaction with CH_3 to produce the target product.

To better elucidate the reaction mechanism involved, future work will focus on gaining a detailed understanding how CF_2 interacts with alumina surfaces. Further research efforts will also be directed toward searching for other methods for activation of CH_4 in order to enhance selectivity and yield to $C_2H_2F_2$.

Acknowledgements

Australian Research Council is gratefully acknowledged for financial support of this project. Authors also wish to thank Yong Joon Lee at the University of New South Wales, Australia for help with BET surface area measurement.

Literature Cited

1 The Freedonia Group, In., Fluorochemicals Industry Study with Forecasts to 2007 & 2012, http://www.freedoniagroup.com/World-Fluorochemicals.html.

2 U. S. EPA, Greenhouse Gases and Global Warming Potential Values, see the PDF file (ghg_gwp.pdf) in http://yosemite.epa.gov/oar/globalwarming.nsf/UniqueKeyLookup /SHSU5BUM9T.

3 Moon, D. J.; Chung, M. J.; Kim, H.; Kwon, Y. S.; Ahn, B. S. Pyrolysis of Trifluoromethane to Produce Hexafluoropropylene**.** *Ind. Eng. Chem. Res.*, **2002**, *41*, 2895-2902.

4 Nagasaki, N; Morikuni, Y; Kawada K.; Arai, S. Study on a Novel Catalytic Reaction and its Mechanism for CF_3I Synthesis. *Catal. Today*, **2004**, *88*, 121-126.

5 Uddin, M. A.; Kennedy, E. M.; Dlugogorski, B. Z. Gas-Phase Reaction of CCl_2F_2 (CFC-12) with Methane. *Chemosphere* **2003**, *53*, 1189-1191.

6 Yu, H.; Kennedy, E. M.; Mackie, J. C.; Dlugogorski, B. Z. Experimental and Computational Studies of Reaction of Halon 1211 ($CBrClF_2$) With Methane, *The 15th Proceedings of Halon Options Technical Working Conference (HOWC)*, Albuquerque, NM, May 24-26, 2005. (also available at http://fire.nist.gov/bfrlpubs/fire05/art083.html).

7 Li, K.; Kennedy, E. M.; Dlugogorski, B. Z. Gas-Phase Reaction of Halon 1301 ($CBrF_3$) with Methane. *Ind. Eng. Chem. Res.*, **1999**, *38*, 3345-3352.

8 Yu, H.; Kennedy, E. M.; Uddin, M. A.; Dlugogorski, B. Z. Catalytic Hydrodehalogenation of Halon 1211 ($CBrClF_2$) over Carbon-Supported Palladium Catalysts. *Appl. Catal. B* **2003**, *44*, 253-261.

9 Kee, R. J.; Rupley, F. M.; Miller, J. A.; Coltrin, M. E.; Grcar, J. F.; Meeks, E.; Moffat, H. K.; Lutz, A. E.; Dixon-Lewis, G.; Smooke, M. D.; Warnatz, J.; Evans, G. H.; Larson, R. S.; Mitchell, R. E.; Petzold, L. R.; Reynolds, W. C.; Caracotsios, M.; Stewart, W. E.; Glarborg, P.; Wang, C.; Adigun, O.; Houf, W. G.; Chou, C. P.; Miller, S. F. Chemkin Collection, Release 3.7, Reaction Design, Inc.: San Diego, CA.

10 Hidaka, Y: Nakamura, T; Kawano, H. High-Temperature Pyrolysis of Trifluoromethane in Shock Waves. *Chem. Phys. Lett.*, **1991**, *187*, 40-44.

11 NIST, WWW CKMech NIST Mechanisms, http://www.cstl.nist.gov/div836/ckmech/nisthfc.html.

12 Smith, G. P.; Golden, D. M.; Frenklach, M.: Moriarty, N. W.: Eiteneer, B.; Goldenberg, M.; Bowman, C. T.; Hanson, R. K.; Song, S.; Gardiner, W. C.; Lissianski, Jr. V. V.; Qin, Z. GRI-Mech 3.0, http://www.me.berkeley.edu/gri_mech/.

13 Yu, H.; Mackie, J. C.; Kennedy, E. M.; Dlugogorski, B. Z. Quantum Chemical Study of the Reaction $CF_2 + CH_3 \leftrightarrow CF_2CH_3 \rightarrow CH_2{=}CF_2 + H$: A Key Mechanism in the Reaction Between ethane and Fluorocarbons, *Ind. Eng. Chem. Res.* (in press)

14 Battin-Leclerc, F.; Smith, A. P.; Hayman, G. D.; Murrells, T. P. Kinetics of the Self-Reaction of CF_2 Radical and its Reaction with H_2, O_2, CH_4 and C_2H_4 over the Temperature Range 295-873 K.*J. Chem. Soc., Faraday Trans*., **1996**, *92*, 3305-3313.

15 Benson, S. W. *Thermochemical Kinetics: Methods for the Estimation of Thermochemical Data and Rate Parameters*, John Wiley & Sons, In.: New York, 1968.

16 Bankhead, M.; Watson, G. W.; Hutchings, G. J.; Scott, J.; Willock, D. J. Calculation of the Energy Profile for the Fluorination of Dichloromethane over an α-Alumina Catalyst. *Appl. Catal. A*, **2000**, *200*, 263-274.

17. Hess, A.; Kemnitz, E.; Lippitz, A.; Unger, W. E. S.; Menz, D. H. ESCA, XRD, and IR Characterisation of Aluminum Oxide, Hydroxyfluoride, and Fluoride Surfaces in Correlation with Their Catalytic Activity in Heterogeneous Halogen Exchange Reactions. *J. Catal.* **1994**, *148*, 273-80.

18 Alonso, C.; Morato, A.; Medina, F.; Cesteros, Y.; Salagre, P.; Sueiras, J. E. Effect of the Aluminum Fluoride Phase for the Cl/F Exchange Reactions in CCl_2F_2 (CFC-12) and $CHClF_2$ (HCFC-22). *Appl. Catal. B*, **2003**, *40*, 259-269.

19 Buravtsev, N. N.; Grigor'ev, A. S.; Kolbanovskii, Y. A. Kinetics of Formation and Decomposition of Perfluorobutenes during Gas-Phase Pyrolysis of Lower Perfluoro Olefins. *Kinet. Katal.*, 1989, **30**, 449-453.

20 Bozzelli, J. W.; Ritter, E. R. THERM version 4.5, 1994.

21 Yaws, C. L. *Chemical Properties Handbook: Physical, Thermodynamic, Environmental, Transport, Safety, and Health Related Properties for Organic and Inorganic Chemicals*, McGraw-Hill: New York, 1999.